

# Design Automation for RF Front End Optimization

Jaakko Juntunen<sup>1</sup>, Joni Lappalainen<sup>1</sup> and Jussi Rahola<sup>1</sup>

<sup>1</sup>Optenni Ltd, Finland

## Introduction

A fundamental functional block in all smartphones in the world is RF front end (RF FE). It can be considered as the busy hub that channels all incoming and outgoing signals precisely to the right place, to the antennas for transmission or to the transceiver RFIC for reception. It is difficult to overestimate the importance of RF FE, as its contribution to the performance of the smartphone is indispensable.

The burning issue in the mobile communication technology is the demand for higher data transfer rates and network capacity. From a single user perspective this translates essentially to requirement of more bandwidth, while from the network infrastructure perspective there are other aspects as well, such as spatial channel re-allocation planning and active beam steering at base station antennas.

Optimal use of the available communication channels at any specific location and time requires a dynamic communication system: the number of mobile terminals in a network cell varies, the demand for data transfer varies from user to user, and the best possible resource allocation is a very complicated problem that calls for dynamic re-allocation of channels. To facilitate the bandwidth allocation, many smartphones already support the so-called carrier aggregation (CA) technologies, where the handset can dynamically switch to transmitting data on several frequency bands simultaneously. This enables temporary multiplication of the data transmit capacity for e.g. downloading a video or a large document.

When it comes to actual implementation of the carrier aggregation technologies in the RF front end, significant new challenges arise related to the implementation of filters in a dynamically changing impedance environment. In this article we elaborate on some of these challenges and propose a design methodology that can process massive amount of circuit-level candidate solutions automatically, lifting a heavy load from the designer's shoulders and revealing feasible solutions relatively easily.

## What is the design challenge?

Figure 1 shows a simplified block diagram of one possible architecture of a two-way inter-band downlink carrier aggregation (DL CA) system, where RX branch for Band 3 may dynamically be connected in parallel with the TX/RX branch of Band 1. One can easily expand the idea for multiple component carriers and different switching configurations. For example Infineon Technologies Application Guide for Mobile Communication ([www.infineon.com/appguide\\_rf\\_mobile](http://www.infineon.com/appguide_rf_mobile)) suggests single- and dual-antenna downlink RF FE architectures supporting up to 5 CA component carriers. The fundamental building blocks are switches, duplexers and bandpass filters – all of which are well known, high quality and widely used in mobile phones – so the question arises if there is any particular problem beyond the choice of the architecture and handling of the frequency planning regarding intermodulation?

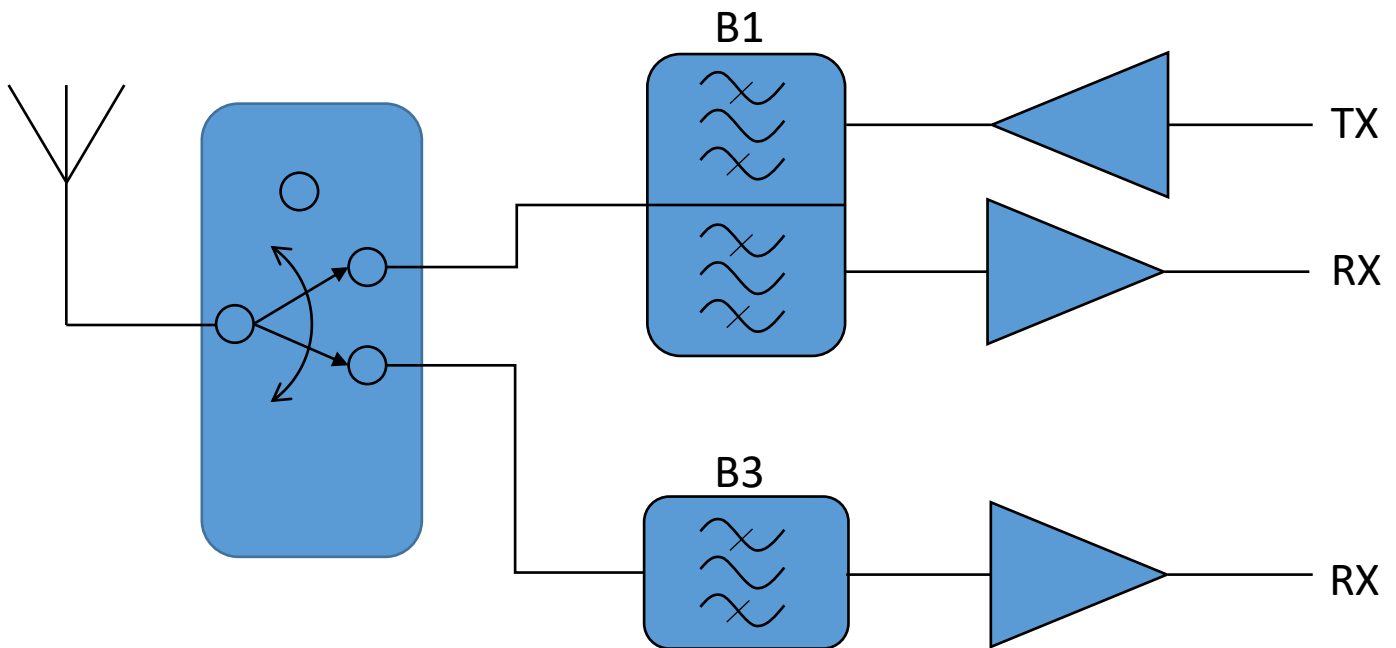


Figure 1. Simplified block diagram of a single-antenna two downlink band carrier aggregation principle in RF front end.

Unfortunately, the answer is yes: there is a significant design bottleneck arising from the fact that filters cannot be connected in parallel without *significantly* affecting each other's performance. As an example, Figure 2 shows the frequency response of sample Band 8 and Band 1 filters separately and when connected into a common node. Remarkably, the Band 1 filter performance is entirely destroyed by the presence of Band 8 filter, while Band 8 filter performance is essentially not changed by the presence of Band 1 filter. Let us analyze the reason for that.

Both filters have very good out of the band rejection, so a possible filter leak does not explain the ruining of Band 1 filter. But when we look the input impedance of Band 8 filter at the Band 1 frequencies in Figure 3a, we notice that instead of an open circuit, Band 8 filter looks like an open-ended transmission line of about 67 degrees of electrical length. When connected into a common node with the Band 1 filter, the Band 8 filter then loads the Band 1 filter performance in a similar fashion as an open stub, which changes entirely the filter performance!

We may already guess why Band 8 filter performance was not spoiled by the presence of Band 1 filter. If we look at Band 1 filter input impedance at Band 8 frequencies (Figure 3b), we notice that Band 1 filter looks essentially like an open circuit *by good luck*. This motivates a practical goal to design matching circuits (phase shifters) that preserve the filter passband behavior but maps the response at the other component carrier frequencies into an open circuit. If this goal is successfully achieved, the filters are transparent to each other and can be connected in any CA configuration. Let us call this part of the design process “filter co-matching”.

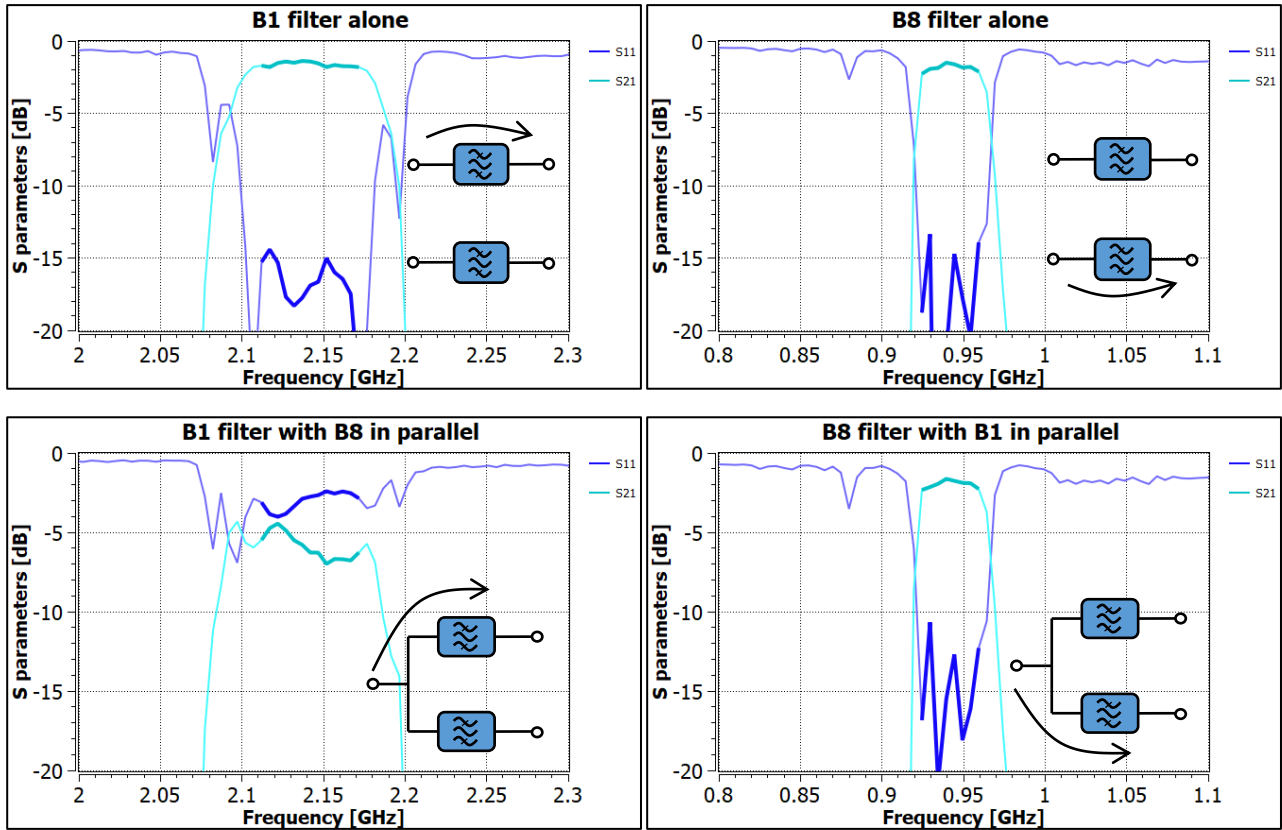
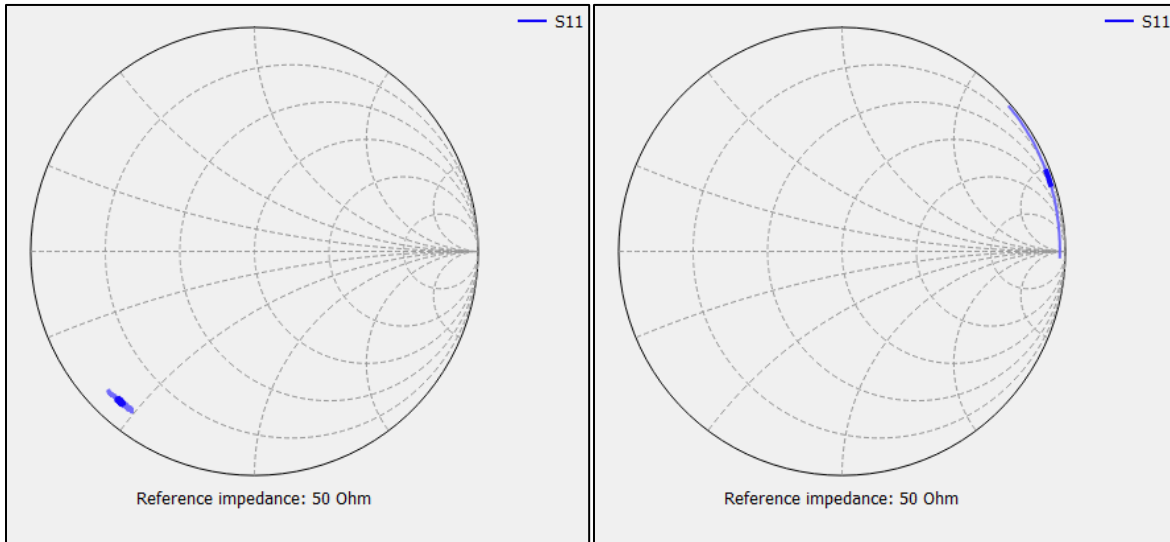


Figure 2. Band 1 and Band 8 filter performance in isolation (top row) and when connected into a common node (bottom row).



Figures 3a and b. Band 8 filter input impedance (left) at Band 1 frequencies looks like  $\sim 67$  degrees long open-ended transmission line, whereas Band 1 filter input impedance (right) at Band 8 frequencies looks nearly like an open circuit, thus not influencing Band 8 filter performance when connected in parallel.

### Challenges in solving the filter co-matching problem

When seeking co-matched solutions, a more or less perfect solution is found only occasionally. This is usually the case with component carriers with wide frequency separation, for example between low-band (LB) and high-band (HB) pairs. The mutual open circuit is more difficult to achieve, when more than one component carrier frequency must be mapped onto an open circuit. Moreover, component carriers at nearby frequencies may be very difficult to co-match without significantly influencing the passband behavior. Furthermore, there is often a practical, conflicting constraint to keep the number of external matching components very small. Therefore, it is desirable to design the acoustic filters upfront such that they allow certain CA scenarios with only few matching components, but there are not enough design degrees of freedom in the filters that would entirely remove the need for external matching.

So we are left with the design process where the co-matching is first attempted, and if it is successful, we know that the CA basically works. In the design process using filter co-matching we often have to accept solutions which do not provide an exact open circuit at the component carrier frequencies, leaving an amount of interaction and loading between the filters. Referring to Figure 1, we also have the switch that connects these interactions, and the electrical dimensions of the switches are large enough that they also contribute to the effective loading on one filter to the other.

These challenges together call for a fine-tuning step with a complete model that involves the switch, the filters and the external matching circuits.

### Example: Band 1 + Band 3 downlink carrier aggregation

Let us consider the case of Figure 1 in detail, where the component carrier bands are relatively close to each other. We use representative public domain S-parameter models for Band 1 duplexer and Band 3 RX filter, as well as a generic semiconductor SP2T model supporting parallel throw state. In the non-CA configuration, the

switch connects the antenna to the Band 1 branch and in the CA configuration, the switch connects the antenna to both the Band 1 and Band 3 branches. The matching circuits should be thus optimized to work with both of these configurations. Let us assign the switch RF1 node for Band 1 and RF2 node for Band 3, and design the matching circuits using 0201 package size Murata discrete component models from libraries LQW03AW\_00 (inductors) and GJM03 (capacitors).

Let us first try to co-match Band 3 filter. For all the matching tasks we use RF design automation software platform Optenni Lab, as it synthesizes and optimizes automatically a big number of candidate topologies. This is an essential remedy: even with only up to 2 matching components there are 17 different topology alternatives *per circuit*, and when there are no obvious solutions for good co-matching, it is in general difficult to prejudge which topology combination provides the best performance. As an example, for a single duplexer there are  $17^3=4913$  different topologies, if each branch is allowed to have up to 2 matching components. Majority of the topologies are doomed to fail, but there can easily be more than 100 relevant topologies which the RF design automation software platform optimizes and ranks automatically, also taking into account the solution sensitivity to component tolerances. This is very helpful, making it less likely to miss the best performing and most tolerance robust topology combination – which could easily happen if only a few topologies are studied manually.

We thus take Band 3 filter model and synthesize matching circuits with the open circuit target at Band 1 frequencies, and good insertion loss target at Band 3 RX. Because Band 1 and Band 3 are quite close to each other, we face the co-matching challenge: Band 1 frequencies span a long arc on Smith chart edge, and attempting to localize it close to the open circuit point can only be done with considerable compromise to the passband response. There are many topologies that we could choose, some of them have better insertion loss, some of them map better onto open circuit – the choice is more or less ambiguous. The impedance at Band 3 RX and Band 1 are shown in Figure 4, comparing the unmatched and our choice of co-matched filter, comprising of 3 matching components on the input side of the filter, and 2 components on the output side.

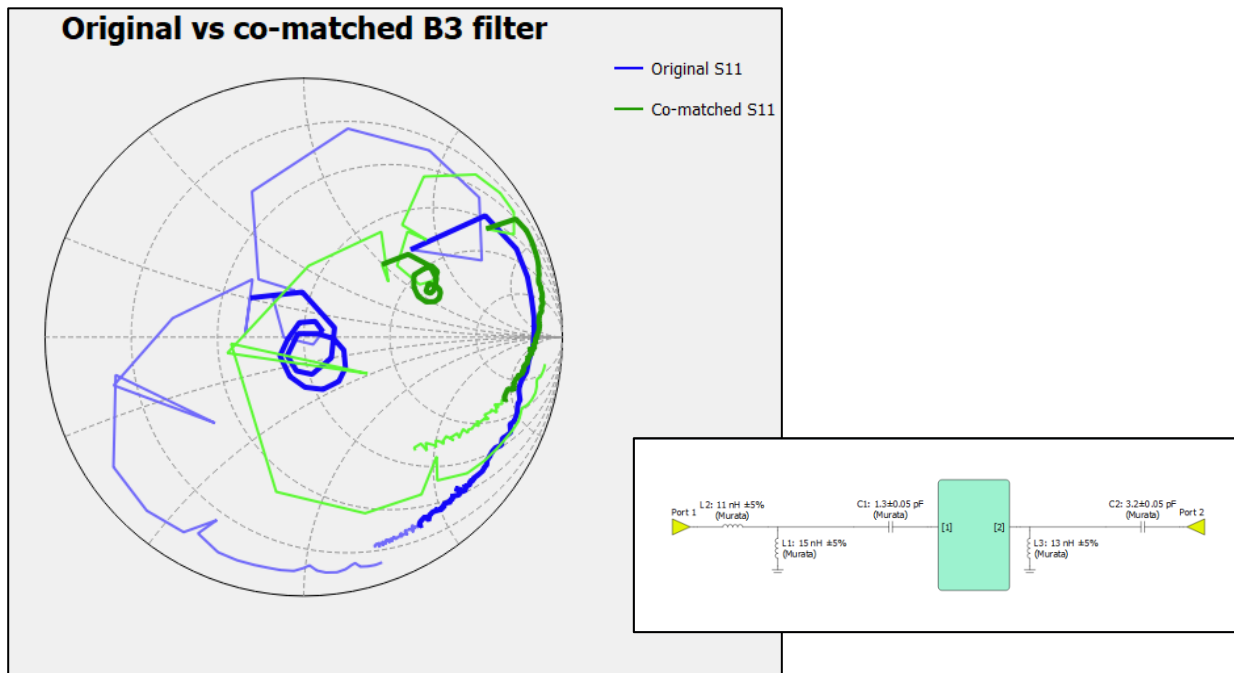


Figure 4. Input impedance of unmatched (blue) and co-matched (green) Band 3 filter. The switch is connected to port 1 on the left, and port 2 is connected to the receiver node on the right.

Regarding the Band 1 duplexer, it turns out more straightforward to pick a circuit with reasonable compromise between TX/RX path insertion losses and Band 3 co-matching. Two components on each branch is required, and the resulting impedance at antenna node of the duplexer is shown in Figure 5.

We can now combine these circuits with the switch model as sketched in Figure 6, and check the performance with the given topologies and component values. The results are given in Figure 7. We can see that the performance is not super great, but still better than without the matching circuits, especially in CA configuration. Note that for this solution we are using a total of 11 matching components. Simply re-optimizing these component values results in significant improvement to the signal path insertion losses in both non-CA and CA configurations. This means that the method where individual filters are first co-matched and then combined in a CA configuration provides a good topology candidate, but the matching component values must be re-optimized. Note that the optimization target is now the minimization of the signal path insertion losses between the switch common node and the active Tx/Rx nodes together with keeping the desired filter rejection between the bands. Different targets are set for the non-CA and CA configurations, where also the switch state changes between the configurations.

However, it is also possible to start from the combined diagram upfront with the switch, duplexer and filter in place, and have the matching circuits as black boxes in respective locations. The RF design automation software platform then synthesizes many new topology combinations for the signal path insertion loss and rejection targets, without considering the intermediate co-matching problems separately. This allows the designer to seek the simplest topologies that still perform sufficiently well by simply inspecting the list of synthesized topologies. Let us call this approach “full-diagram optimization”.

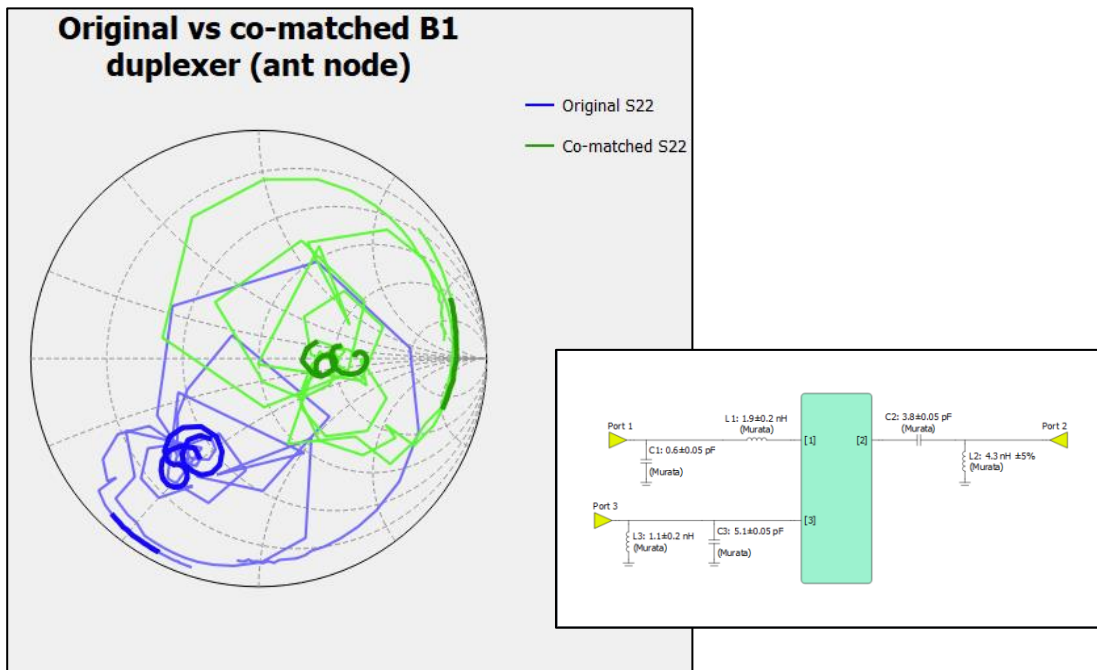


Figure 5. Antenna node impedance of unmatched (blue) and co-matched (green) Band 1 duplexer. Port 1 = TX, Port 2 = ant node (connected to switch), Port 3 = RX.

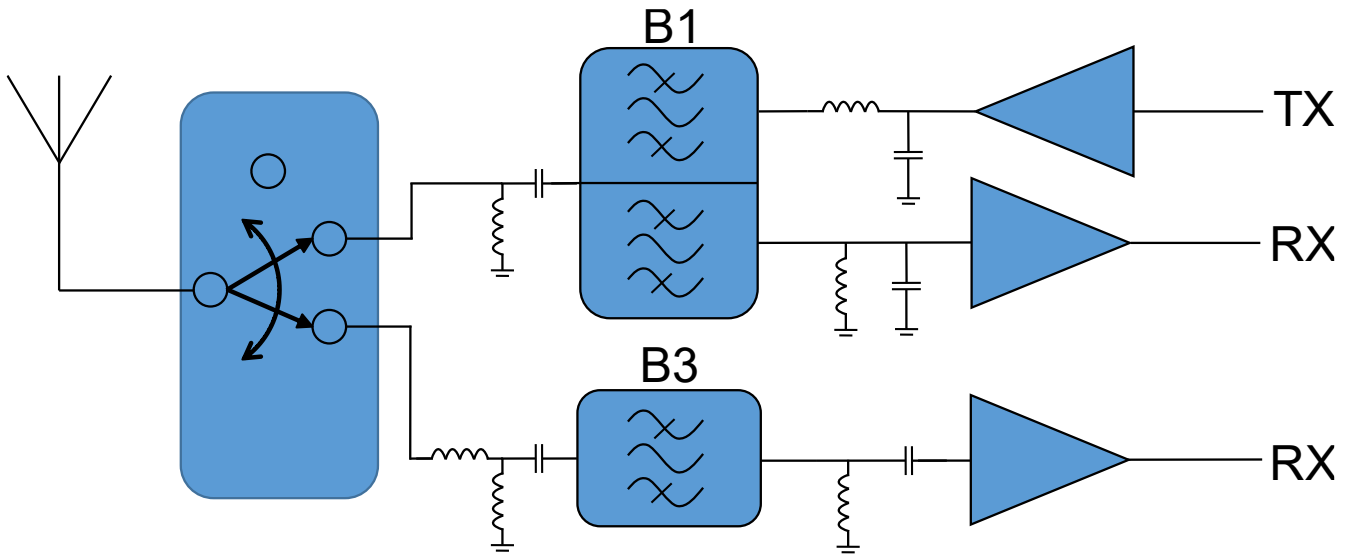


Figure 6. Co-matched B1 duplexer and B3 filter combined with the switch. 11 matching components.

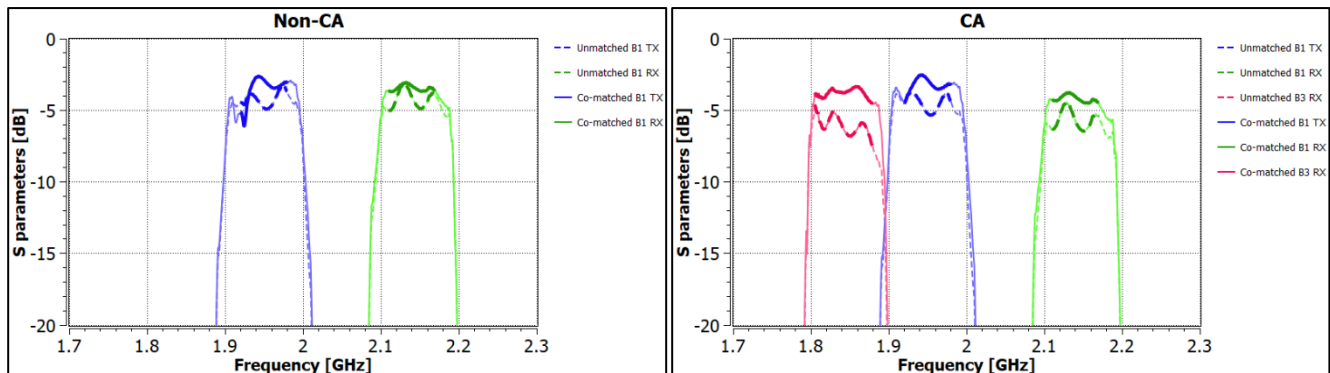


Figure 7. Signal insertion losses of non-CA and CA configurations with unmatched and co-matched filters.

It turns out that we can achieve practically speaking the same performance with only *eight* matching components as was achieved using the filter co-matching as an intermediate step (with 11 matching components). The sketch of the optimal matching circuitry is shown in Figure 8 and the corresponding results are shown in Figure 9, together with the results of optimized 11-component circuitry. To quantify the performance of the circuitry (including the switch) we can introduce a metric “CA matching efficiency” that represents the insertion loss degradation in CA mode when compared to *isolated* duplexer/filter, i.e. using as a reference the individual signal insertion losses in architecture that does not support CA at all. The results are: -1.2 dB for B1 RX, -0.7 dB for B1 TX and -1.3 dB for B3 RX, averaging to about -1.0 dB. This figure of merit indeed includes the switch loss, which is about 0.4 dB in this case. It is also to be noted that the B1 duplexer model used in this study is not prematched, and the nominal, isolated performance already requires two matching components, so the true matching component count overhead for the whole CA configuration is only six.

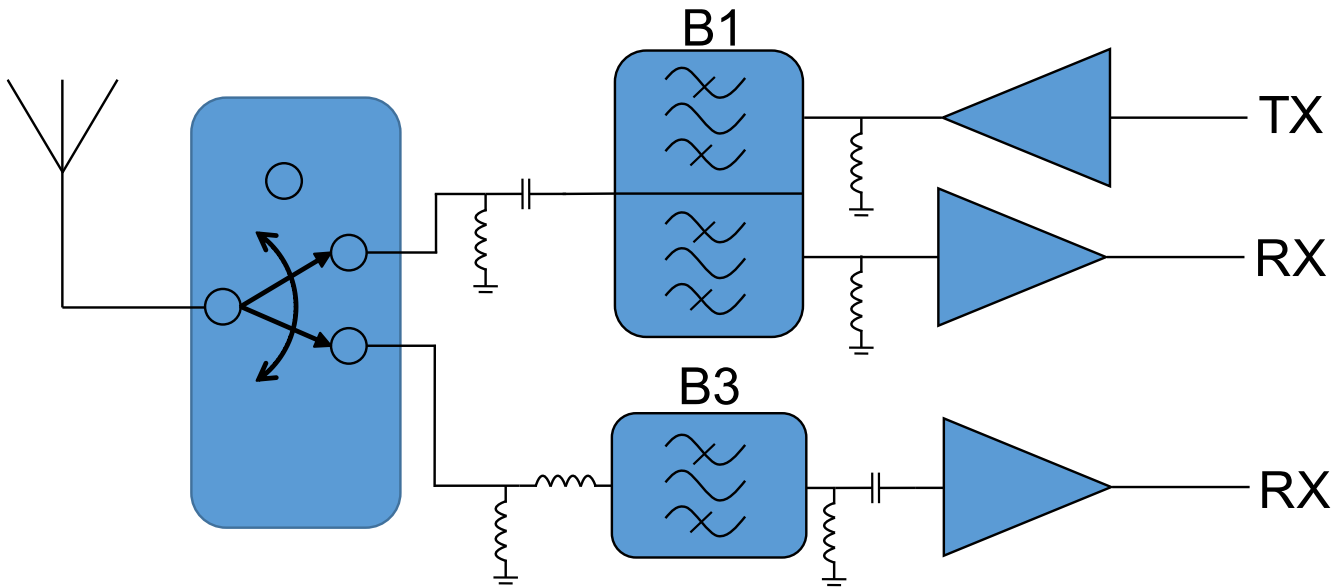


Figure 8. Optimal matching topology resulting from full-diagram optimization. 8 matching components.

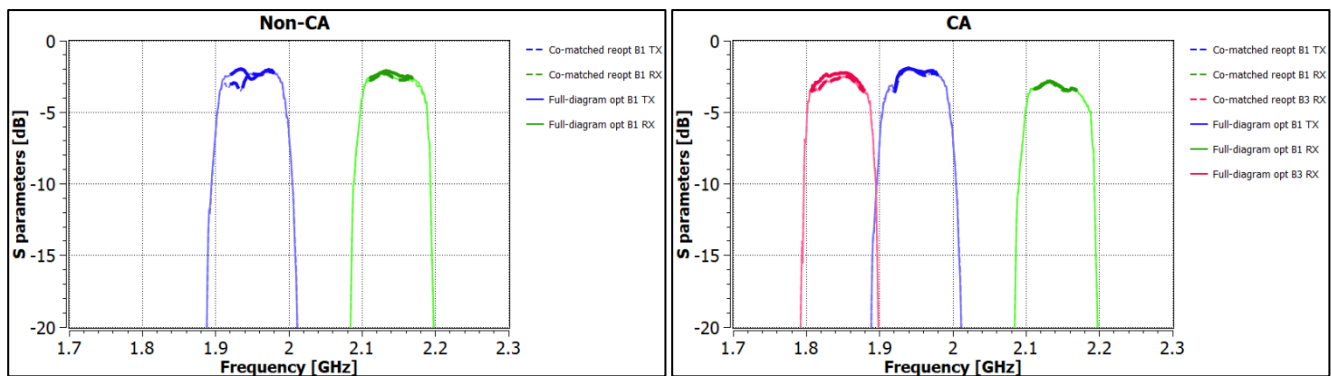


Figure 9. Signal insertion losses of non-CA and CA configurations due to optimized filter co-matching approach and full-diagram optimization approach. The performance is almost equal.

## Conclusions

The benefits of carrier aggregation are obvious from the mobile communication system perspective, but unfortunately the realization of CA architectures involves significant design challenges. These challenges emerge from the fact that when filters for different frequency bands are connected into a common node, they influence the performance of each other, often spoiling the basic filter performance completely. This can be rectified by designing auxiliary matching circuits that map the filters mutually onto open circuit, thus making the filters invisible to each other.

In this article we compare two approaches for the matching of the CA filters. In the “co-matching” approach, the filters are first matched separately, with the target of obtaining an open circuit at the frequency of the other filter. When the results of such subproblems are combined and fine-tuned, we typically get a working solution.



However, this process provides basically just one matching topology, or requires laborious manual combination of the results of the subproblem candidates. Therefore, we propose a second method that we call “full-diagram optimization”, which omits the co-matching step and searches optimal circuits directly to the actual performance metric, i.e. the signal insertion losses and rejections. This allows identification of the most economical solution very efficiently. Practical, more complex CA architectures may benefit from a hybrid approach where some functional blocks are designed using “full-diagram optimization”, but then combined together and fine-tuned, similar to “co-matching” approach. In all these approaches the automated topology synthesis of the used RF design automation platform is a key part, because it eliminates a major portion of the manual work that the designer otherwise had to spend on design software while solving the CA problem.